

DIFFERENCE APPROXIMATIONS FOR THE SECOND ORDER WAVE EQUATION*

HEINZ-OTTO KREISS[†], N. ANDERS PETERSSON[‡], AND JACOB YSTRÖM[§]

Abstract. Difference approximations are derived for the second order wave equation in one and two space dimensions, without first writing it as a first order system. Both the Dirichlet and the Neumann problems are treated for the one-dimensional case. Relations between the boundary error and the interior phase error are derived for a fully second order accurate discretization as well as a scheme that is fourth order accurate in the interior and second order accurate at the boundary. General two-dimensional domains are considered for the Dirichlet problem where the domain is embedded in a Cartesian grid and the boundary conditions are approximated by interpolation. A stable conservative scheme is derived where the time step is determined only by the interior discretization formula. Discretization cells cut by the boundary are treated implicitly, but the resulting scheme becomes explicit because the implicit dependence only is pointwise. Numerical examples are provided to verify the stability and accuracy of the proposed method.

Key words. wave equation, stability, accuracy, embedded boundary

AMS subject classifications. 65M06, 65M12

PII. S0036142901397435

1. Introduction. The theory of difference approximations for first order strongly hyperbolic systems is by now very well developed. However, in many applications like seismology, acoustics, and general relativity the underlying differential equations are systems of second order hyperbolic partial differential equations. It is surprising that in this case the corresponding theory is much less developed. Instead, one often rewrites the equations as a first order system and then uses methods developed for such systems. While these methods provide the most natural way to solve problems that come as first order systems, we will argue that there can be drawbacks with rewriting second order systems into this form before they are discretized. Instead, we propose a numerical method that directly discretizes the second order system.

Consider, for example, the wave equation

$$(1.1) \quad u_{tt} = u_{xx}$$

in the strip $0 \leq x \leq 1$, $t \geq 0$. Thus we have to give initial conditions

$$(1.2) \quad u(x, 0) = f(x), \quad u_t(x, 0) = g(x),$$

and boundary conditions, for example,

$$(1.3) \quad u(0, t) = h_0(t), \quad u(1, t) = h_1(t).$$

*Received by the editors November 2, 2001; accepted for publication (in revised form) April 30, 2002; published electronically December 3, 2002. This work was performed under the auspices of the U.S. Department of Energy by University of California Lawrence Livermore National Laboratory under contract W-7405-Eng-48.

<http://www.siam.org/journals/sinum/40-5/39743.html>

[†]Department of Mathematics, University of California, Los Angeles, CA 90024 (kreiss@math.ucla.edu).

[‡]Center for Applied Scientific Computing, Lawrence Livermore National Lab, Livermore, CA 94551 (andersp@llnl.gov).

[§]Department of Numerical Analysis and Computing Science, Royal Institute of Technology, S-100 44 Stockholm, Sweden (yxan@nada.kth.se).

To solve the problem numerically, we introduce a grid by

$$t_n = nk, \quad k > 0, \quad n = 0, 1, 2, \dots, \quad x_\nu = \nu h, \quad h = 1/N, \quad \nu = 0, 1, 2, \dots, N,$$

and approximate (1.1)–(1.3) by a completely centered approximation

$$(1.4) \quad \begin{aligned} D_+^t D_-^t v(x_\nu, t_n) &= D_+^x D_-^x v(x_\nu, t_n), \quad \nu = 1, 2, \dots, N - 1, \\ v(x_\nu, 0) &= f(x_\nu), \quad v(x_\nu, k) = f(x_\nu) + kg(x_\nu) + \frac{k^2}{2} D_+^x D_-^x f(x_\nu), \\ v(0, t_n) &= h_0(t_n), \quad v(1, t_n) = h_1(t_n). \end{aligned}$$

Here

$$\begin{aligned} hD_+^x v(x_\nu, t) &= v(x_{\nu+1}, t) - v(x_\nu, t), \\ hD_-^x v(x_\nu, t) &= v(x_\nu, t) - v(x_{\nu-1}, t), \\ D_0^x &= \frac{1}{2}(D_+^x + D_-^x) \end{aligned}$$

denote the usual forward, backward, and centered difference operators. As we will see, this approximation and its generalization to more space dimensions work very well. There are no difficulties with the boundary conditions; i.e., we do not need to supply any extrapolation conditions.

One can write (1.1) as a first order system

$$(1.5) \quad \mathbf{u}_t = A\mathbf{u}_x, \quad \mathbf{u} = \begin{pmatrix} u \\ v \end{pmatrix}, \quad A = \begin{pmatrix} 0 & 1 \\ 1 & 0 \end{pmatrix}$$

with initial conditions

$$\mathbf{u}(x, 0) = \mathbf{f}, \quad \mathbf{f} = \left(f, \int_0^x g(\tilde{x}) d\tilde{x} \right)^T,$$

and boundary conditions (1.3). The leap-frog scheme is often used to solve wave propagation problems. For (1.5) it is, in its simplest form, given by

$$(1.6) \quad \begin{aligned} D_0^t \mathbf{u}(x_\nu, t_n) &= AD_0^x \mathbf{u}(x_\nu, t_n), \quad \nu = 1, 2, \dots, N - 1, \\ \mathbf{u}(x_\nu, 0) &= \mathbf{f}(x_\nu), \quad \mathbf{u}(x_\nu, k) = \mathbf{f}(x_\nu) + kAD_0^x \mathbf{u}(x_\nu, 0). \end{aligned}$$

There are a number of drawbacks with this procedure:

1. One needs to calculate two variables. (More variables are needed in several space dimensions.)
2. To obtain the same accuracy as (1.4), one needs to double the number of grid points in space and time.
3. Since there are no boundary conditions for v , one has to supply extrapolation conditions to obtain $v(0, t)$ and $v(1, t)$. This can be done, but one has to be careful not to introduce instabilities; see [5].
4. If the solution is not properly resolved, i.e., if one does not use enough points/wavelength, then one creates spurious waves which travel in the wrong direction; see [1].

To avoid the three latter difficulties, one may introduce a so-called staggered grid. However, this amounts to nothing else but solving (1.4) in disguise. In more space dimensions, staggered grids can lead to complications at the boundaries.

In the present paper, we directly approach the wave equation as a second order system. The equations are discretized on a Cartesian grid that covers the domain of interest, and the spatial derivatives are approximated by finite differences. On the boundary, which is embedded in the Cartesian grid, we use interpolation to approximate the boundary condition. This procedure results in a closed second order system of ordinary differential equations, and we derive an appropriate time-integration method for this system.

Numerical methods for first order systems are by now well developed, and many useful techniques have been established, such as higher order accurate boundary conditions [9], accurate treatment of discontinuous coefficients [4], and nonreflecting boundary conditions for external domains. The method presented here currently lacks these refinements, so a direct comparison on a realistic problem is hard to make. Instead, this work should be seen as a starting point for the development of a numerical technique that directly approaches second order hyperbolic systems.

Embedded boundary techniques for discretizing Laplace's equation subject to Dirichlet boundary conditions date back to Weller and Shortley [10], who used a finite-volume method (perhaps before that term was coined) to set up first order accurate difference approximations near the boundary. Collatz [2] derived higher order difference methods for both the Neumann and Dirichlet problems. More recently, several embedded boundary methods have been presented for various types of partial differential equations. For example, Pember et al. [8] used a Cartesian grid method for solving the time-dependent equations of gas dynamics. Zhang and LeVeque [11] solved the acoustic wave equation with discontinuous coefficients written as a first order system. They derived special difference stencils that satisfy the jump conditions at the interior interfaces, where the coefficients are discontinuous. A staggered grid method was used by Ditkowski, Dridi, and Hesthaven [3] for solving Maxwell's equations on a Cartesian grid. The methods described in these papers all solve first order systems (in time). Johansen and Colella [6] derived a finite-volume scheme for solving Poisson's equation with Dirichlet boundary conditions using an embedded boundary technique. Away from the boundary, the truncation error for the Laplace operator is $O(h^2)$, but in cells cut by the boundary it becomes $O(h/\Gamma)$. (Here h is the mesh spacing and Γ is the area fraction of the cut cell.) A potential theoretic argument is used to show that the solution of Poisson's equation is still second order accurate, even as $\Gamma \rightarrow 0$. However, the large truncation error in cells cut by the boundary makes this method unsuitable for solving the wave equation, where the truncation error for the Laplace operator also needs to be small near the boundary.

We shall now summarize the remainder of the paper. In section 2 we discuss a second order accurate time-integration method to solve the system of ordinary differential equations that arises after the wave equation is discretized in space. In particular, we derive a semi-implicit approach to avoid the severe time-step restriction that otherwise can occur from small cells cut by the boundary. When certain symmetry conditions are satisfied, the time-integration method is shown to be stable and conservative.

Section 3 contains a discussion of the stability and accuracy of semidiscrete approximations in one space dimension both for Dirichlet and Neumann boundary conditions. We consider methods that are second order accurate overall and methods

that are fourth order accurate in the interior and second order accurate at the boundary. Analytically, we derive the relation between the boundary error and the interior phase error. The analysis clearly shows that for the second order accurate method, the phase error dominates if we integrate over long distances. By using the fourth order method in the interior, we show that the phase error is greatly reduced.

The Dirichlet problem for the wave equation in general two-dimensional domains is treated in section 4. We show that we can construct stable energy conserving schemes that are either second order accurate overall or second order accurate at the boundary and fourth order accurate in the interior. We show that the scheme can be derived “dimension by dimension”, essentially by employing the one-dimensional scheme in each direction. Since the semi-implicit treatment of the cut cells at the boundary is pointwise, the resulting scheme is fully explicit and therefore highly effective.

Numerical examples are provided in section 5, where we solve the two-dimensional Dirichlet problem to demonstrate the accuracy and stability of the proposed method. Future research is outlined in section 6.

2. Ordinary differential equations. Consider the initial value problem for the scalar equation

$$(2.1) \quad u_{tt} = \lambda u + F(t)$$

with initial conditions

$$(2.2) \quad u(0) = u_0, \quad u_t(0) = u_1.$$

Here $F(t)$ is a smooth function and $\lambda < 0$ is a negative constant.

The usual way to solve (2.1), (2.2) numerically is to rewrite the equation as a first order system and then apply any of the standard schemes. In this paper we solve the equation directly. Let k be the time step, $t_n = nk$, and denote the discrete approximation $v^n \approx u(t_n)$. We use two different second order accurate schemes:

1. If $\lambda \sim -1$, we use

$$(2.3) \quad v^{n+1} - 2v^n + v^{n-1} = k^2(\lambda v^n + F(t_n)).$$

2. If $\lambda \ll -1$, then we use instead

$$v^{n+1} - 2v^n + v^{n-1} = k^2 \left(\frac{\lambda}{2}(v^{n+1} + v^{n-1}) + F(t_n) \right).$$

The last method can also be written as

$$(2.4) \quad \left(1 - \frac{\lambda k^2}{2} \right) (v^{n+1} - 2v^n + v^{n-1}) = \lambda k^2 v^n + k^2 F(t_n).$$

We initialize the schemes by

$$v_0 = u_0, \quad v_1 = u(0) + k u_t(0) + \frac{k^2}{2} u_{tt}(0) = u_0 + k u_1 + \frac{k^2}{2} (\lambda u_0 + F(0)).$$

The characteristic equations for (2.3) and (2.4) are given by

$$(\kappa - 1)^2 - k^2 \lambda \kappa = 0, \quad \left(1 - \frac{\lambda k^2}{2} \right) (\kappa - 1)^2 - \lambda k^2 \kappa = 0,$$

respectively. Thus,

$$\kappa = 1 + \frac{1}{2}\zeta \pm \sqrt{\zeta + \frac{1}{4}\zeta^2},$$

where

$$\zeta = \lambda k^2 \quad \text{for (2.3)} \quad \text{and} \quad \zeta = \frac{\lambda k^2}{1 - \lambda k^2/2} \quad \text{for (2.4)}.$$

Thus, $|\kappa_1| = |\kappa_2| = 1$, $\kappa_1 \neq \kappa_2$, for $-4 < \zeta < 0$. Hence, the approximation (2.3) is stable for $k < 2/\sqrt{-\lambda}$, while the scheme (2.4) is unconditionally stable.

Now we consider systems

$$(2.5) \quad \begin{aligned} \mathbf{u}_{tt} &= A\mathbf{u} + F(t), \\ \mathbf{u}(0) &= \mathbf{u}_0, \quad \mathbf{u}_t(0) = \mathbf{u}_1, \end{aligned}$$

and the corresponding homogeneous problem

$$(2.6) \quad \begin{aligned} \mathbf{v}_{tt} &= A\mathbf{v}, \\ \mathbf{v}(0) &= \mathbf{v}_0, \quad \mathbf{v}_t(0) = \mathbf{v}_1. \end{aligned}$$

LEMMA 2.1. *The solutions of (2.6) are uniformly bounded in time if and only if the eigenvalues of A are real and negative and there is a complete system of eigenvectors.*

Proof. Let λ be an eigenvalue of A and φ_0 the corresponding eigenvector. Then, for any constants σ_1, σ_2 ,

$$\mathbf{v}_\lambda = \begin{cases} (\sigma_1 e^{\sqrt{\lambda}t} + \sigma_2 e^{-\sqrt{\lambda}t})\varphi_0 & \text{if } \lambda \neq 0, \\ (\sigma_1 + \sigma_2 t)\varphi_0 & \text{if } \lambda = 0 \end{cases}$$

is a solution to $\mathbf{v}_{tt} = A\mathbf{v}$. Thus, \mathbf{v}_λ is uniformly bounded in time if and only if λ is real and negative. If there is a complete eigensystem, then we can write the solutions to (2.6) as a sum of eigensolutions. The solutions are therefore uniformly bounded if and only if all the eigenvalues are real and negative.

An easy calculation shows that the solutions of

$$\mathbf{v}_{tt} = J\mathbf{v},$$

where J is a Jordan block, are not uniformly bounded. Therefore, if the eigensystem is incomplete, the solutions of (2.6) are not uniformly bounded. This proves the lemma.

If $A = A^* < 0$ is a negative definite symmetric matrix, then all conditions of the above lemma are satisfied and the solutions are uniformly bounded. We can also prove this by an energy estimate. We have

$$\begin{aligned} \frac{\partial}{\partial t} |\mathbf{v}_t|^2 &= \langle \mathbf{v}_t, \mathbf{v}_{tt} \rangle + \langle \mathbf{v}_t, \mathbf{v}_{tt} \rangle \\ &= \langle \mathbf{v}_t, A\mathbf{v} \rangle + \langle A\mathbf{v}, \mathbf{v}_t \rangle = \frac{\partial}{\partial t} \langle \mathbf{v}, A\mathbf{v} \rangle, \end{aligned}$$

i.e.,

$$(2.7) \quad \frac{\partial}{\partial t} (|\mathbf{v}_t|^2 + \langle \mathbf{v}, (-A)\mathbf{v} \rangle) = 0.$$

Since $-A$ is positive definite, boundedness follows.

We approximate the system (2.6) by

$$t_n = nk, \quad \mathbf{v}^n \approx \mathbf{v}(t_n),$$

and

$$(2.8) \quad \mathbf{v}^{n+1} - 2\mathbf{v}^n + \mathbf{v}^{n-1} = k^2 A \mathbf{v}^n \quad \text{if } |A| \sim 1,$$

$$(2.9) \quad \mathbf{v}^{n+1} - 2\mathbf{v}^n + \mathbf{v}^{n-1} = \frac{k^2}{2} A (\mathbf{v}^{n+1} + \mathbf{v}^{n-1}) \quad \text{if } |A| \gg 1.$$

We can write (2.9) in the form

$$\left(I - \frac{k^2}{2} A \right) (\mathbf{v}^{n+1} - 2\mathbf{v}^n + \mathbf{v}^{n-1}) = k^2 A \mathbf{v}^n.$$

Since we can reduce the system to scalar equations, the difference approximation corresponding to (2.3) is stable if

$$\max_j |\lambda_j| k^2 < 4.$$

The approximation (2.9) is unconditionally stable.

We proceed by using energy methods to derive the discrete counterpart of (2.7) to show that the discrete energy is conserved by the scheme (2.8). We write (2.8) in the form

$$\mathbf{v}^{n+1} + \mathbf{v}^{n-1} = (2I + k^2 A) \mathbf{v}^n.$$

Therefore,

$$\langle \mathbf{v}^{n+1} - \mathbf{v}^{n-1}, \mathbf{v}^{n+1} + \mathbf{v}^{n-1} \rangle = \langle \mathbf{v}^{n+1}, (2I + k^2 A) \mathbf{v}^n \rangle - \langle \mathbf{v}^{n-1}, (2I + k^2 A) \mathbf{v}^n \rangle.$$

Assuming that \mathbf{v}^n, A are real, we obtain

$$\begin{aligned} L(t_{n+1}, A) &= |\mathbf{v}^{n+1}|^2 + |\mathbf{v}^n|^2 - \langle \mathbf{v}^{n+1}, (2I + k^2 A) \mathbf{v}^n \rangle \\ &= |\mathbf{v}^n|^2 + |\mathbf{v}^{n-1}|^2 - \langle \mathbf{v}^n, (2I + k^2 A) \mathbf{v}^{n-1} \rangle \\ &= L(t_n, A). \end{aligned}$$

Thus, we obtain an energy estimate if L is positive definite. We have

$$L(t_{n+1}, A) = \langle \mathbf{v}^{n+1} - \mathbf{v}^n, \mathbf{v}^{n+1} - \mathbf{v}^n \rangle - k^2 \langle \mathbf{v}^{n+1}, A \mathbf{v}^n \rangle.$$

Since $A = A^*$ is symmetric,

$$\langle \mathbf{v}^{n+1}, A \mathbf{v}^n \rangle = \frac{1}{4} \langle \mathbf{v}^{n+1} + \mathbf{v}^n, A(\mathbf{v}^{n+1} + \mathbf{v}^n) \rangle - \frac{1}{4} \langle \mathbf{v}^{n+1} - \mathbf{v}^n, A(\mathbf{v}^{n+1} - \mathbf{v}^n) \rangle.$$

Hence,

$$(2.10) \quad \begin{aligned} L(t_{n+1}, A) &= \left\langle \mathbf{v}^{n+1} - \mathbf{v}^n, \left(I + \frac{k^2}{4} A \right) (\mathbf{v}^{n+1} - \mathbf{v}^n) \right\rangle \\ &\quad - \frac{k^2}{4} \langle \mathbf{v}^{n+1} + \mathbf{v}^n, A(\mathbf{v}^{n+1} + \mathbf{v}^n) \rangle. \end{aligned}$$

Let $\lambda_j < 0$ be the eigenvalues of A . For $4 - k^2 \max_j |\lambda_j| \geq k^2 \min_j |\lambda_j|$,

$$\left\langle \mathbf{v}, \left(I + \frac{k^2}{4} A \right) \mathbf{v} \right\rangle \geq \frac{k^2}{4} \min_j |\lambda_j| |\mathbf{v}|^2$$

and

$$L(t_{n+1}, A) \geq \frac{k^2}{4} \min_j |\lambda_j| (|\mathbf{v}^{n+1} - \mathbf{v}^n|^2 + |\mathbf{v}^{n+1} + \mathbf{v}^n|^2).$$

Thus, $L(t_n, A)$ is positive definite if the time step satisfies

$$(\max_j |\lambda_j| + \min_j |\lambda_j|) k^2 \leq 4$$

and, essentially, we recover the previous time-step restriction.

By comparing (2.11) and (2.7) we note that $L(t_{n+1}, A)/k^2$ is a second order accurate approximation of the energy $|\mathbf{v}_t|^2 - \langle \mathbf{v}, A\mathbf{v} \rangle$, evaluated at time $t_n + k/2$.

Often there are only relatively few elements of A which are large, and we can write

$$A = A_1 + A_2, \quad A_1 = A_1^* \leq 0, \quad |A_1| \gg 1, \quad A_2 = A_2^* < 0, \quad |A_2| \sim 1.$$

To avoid severe restrictions of the step size, we can use the second order approximation

$$(2.11) \quad \mathbf{v}^{n+1} - 2\mathbf{v}^n + \mathbf{v}^{n-1} = \frac{k^2}{2} A_1 (\mathbf{v}^{n+1} + \mathbf{v}^{n-1}) + k^2 A_2 \mathbf{v}^n,$$

which we write as

$$\left(I - \frac{k^2}{2} A_1 \right) (\mathbf{v}^{n+1} - 2\mathbf{v}^n + \mathbf{v}^{n-1}) = k^2 (A_1 + A_2) \mathbf{v}^n$$

or

$$\left(I - \frac{k^2}{2} A_1 \right) (\mathbf{v}^{n+1} + \mathbf{v}^{n-1}) = (2I + k^2 A_2) \mathbf{v}^n.$$

Thus,

$$\left\langle \mathbf{v}^{n+1} - \mathbf{v}^{n-1}, \left(I - \frac{k^2}{2} A_1 \right) (\mathbf{v}^{n+1} + \mathbf{v}^{n-1}) \right\rangle = \langle \mathbf{v}^{n+1} - \mathbf{v}^{n-1}, (2I + k^2 A_2) \mathbf{v}^n \rangle.$$

Similar to the scheme (2.8), we can derive a discrete energy that is conserved. Assuming that \mathbf{v}^n, A_1, A_2 are real, we have

$$\begin{aligned} L_1(t_{n+1}, A_1, A_2) &= \left\langle \mathbf{v}^{n+1}, \left(I - \frac{k^2}{2} A_1 \right) \mathbf{v}^{n+1} \right\rangle + \left\langle \mathbf{v}^n, \left(I - \frac{k^2}{2} A_1 \right) \mathbf{v}^n \right\rangle \\ &\quad - \langle \mathbf{v}^{n+1}, (2I + k^2 A_2) \mathbf{v}^n \rangle \\ &= \left\langle \mathbf{v}^n, \left(I - \frac{k^2}{2} A_1 \right) \mathbf{v}^n \right\rangle + \left\langle \mathbf{v}^{n-1}, \left(I - \frac{k^2}{2} A_1 \right) \mathbf{v}^{n-1} \right\rangle \\ &\quad - \langle \mathbf{v}^n, (2I + k^2 A_2) \mathbf{v}^{n-1} \rangle \\ &= L_1(t_n, A_1, A_2). \end{aligned}$$

We have now to show that $L_1(t_n, A_1, A_2)$ is positive definite. Since $-A_1$ is positive semidefinite,

$$\left\langle \mathbf{v}^{n+1}, -\frac{k^2}{2}A_1\mathbf{v}^{n+1} \right\rangle + \left\langle \mathbf{v}^n, -\frac{k^2}{2}A_1\mathbf{v}^n \right\rangle \geq 0,$$

and it follows that

$$L_1(t_n, A_1, A_2) \geq L(t_n, A_2).$$

Thus $L_1(t_n, A_1, A_2)$ is positive definite since $L(t_n, A_2)$ is positive definite. Hence, the previous time-step restriction applies with A replaced by A_2 . We summarize our results in the following lemma.

LEMMA 2.2. *The time-integration scheme (2.11) is stable and the discrete energy $L_1(t_n, A_1, A_2)$ is conserved if $A_1 = A_1^* \leq 0$, $A_2 = A_2^* < 0$, and the time step satisfies*

$$\left(\max_j |\lambda_j| + \min_j |\lambda_j| \right) k^2 < 4,$$

where λ_j are the eigenvalues of A_2 .

All our results are also valid for systems

$$B\mathbf{u}_{tt} = A\mathbf{u}, \quad A = A^* < 0, \quad B = B^* > 0,$$

because the change of variables $B^{1/2}\mathbf{u} = \tilde{\mathbf{u}}$ gives us

$$\tilde{\mathbf{u}}_{tt} = \tilde{A}\tilde{\mathbf{u}}, \quad \tilde{A} = \tilde{A}^* = B^{-1/2}AB^{-1/2}.$$

3. The wave equation in one space dimension. We consider the wave equation

$$(3.1) \quad u_{tt} = u_{xx}$$

for $x \geq l$, $t \geq 0$. Here $l \geq 0$ is a small number. At $t = 0$ we give initial conditions

$$(3.2) \quad u(x, 0) = f(x), \quad u_t(x, 0) = g(x).$$

Here f is a smooth function with compact support.

3.1. Second order methods. At $x = l$ we give boundary conditions and we start by analyzing Dirichlet conditions

$$(3.3) \quad u(l, t) = 0.$$

Here we discuss second order difference approximations. We only discretize space. In the time direction we use the approximation discussed in the previous section. Let $h > 0$ be a step size. We assume that $l = \alpha h$, $0 \leq \alpha < 1$. Grid points are given by $x_\nu = \nu h$ and grid functions by $w(x_\nu, t) = w_\nu(t)$. We approximate (3.1), (3.2) by

$$(3.4) \quad \begin{aligned} w_{\nu tt} &= D_+ D_- w_\nu, \\ w_\nu(0) &= f_\nu, \quad w_{\nu t}(0) = g_\nu, \quad \nu = 1, 2, \dots \end{aligned}$$

We shall use the simplest second order accurate boundary condition given by the interpolation condition

$$(3.5) \quad \alpha w_1 + (1 - \alpha)w_0 = 0.$$

We can express w_0 in terms of w_1 and eliminate w_0 from (3.4). Then the differential equation for w_1 becomes

$$w_{1tt} = \frac{w_2 - 2w_1 + w_0}{h^2} = \frac{1}{h^2}(aw_1 + bw_2),$$

where

$$a = -\left(2 + \frac{\alpha}{1-\alpha}\right), \quad b = 1.$$

In matrix form (3.4) can be written as

$$\mathbf{w}_{tt} = \frac{1}{h^2} \begin{pmatrix} a & 1 & 0 & 0 & \cdots & 0 \\ 1 & -2 & 1 & 0 & \cdots & \\ 0 & 1 & -2 & 1 & & \\ \vdots & & \ddots & \ddots & \ddots & \\ 0 & & & & & \end{pmatrix} \mathbf{w}, \quad \mathbf{w} = \begin{pmatrix} w_1 \\ w_2 \\ w_3 \\ \vdots \\ \vdots \end{pmatrix}.$$

The matrix is symmetric and negative definite. Since $|a|$ becomes large as $\alpha \rightarrow 1$, we split the matrix and use the scheme (2.11) with

$$A_1 = \frac{1}{h^2} \begin{pmatrix} -\frac{\alpha}{1-\alpha} & 0 & \cdots \\ 0 & 0 & \cdots \\ \vdots & \vdots & \ddots \end{pmatrix}.$$

We now consider Neumann boundary conditions. At $x = \alpha h$ we have

$$u_x(\alpha h) = u_x(0) + \alpha h u_{xx}(0) + \mathcal{O}(h^2).$$

Also,

$$D_+ u_0 = u_x(0) + \frac{h}{2} u_{xx}(0) + \mathcal{O}(h^2).$$

Therefore,

$$u_x(\alpha h) = D_+ u_0 + h \left(\alpha - \frac{1}{2} \right) D_+^2 u_0 + \mathcal{O}(h^2).$$

Thus, we approximate the boundary condition

$$u_x(\alpha h) = 0$$

by

$$(3.6) \quad D_+ w_0 + h \left(\alpha - \frac{1}{2} \right) D_+^2 w_0 = 0,$$

i.e.,

$$\left(\frac{3}{2} - \alpha\right) w_0 = \left(\alpha - \frac{1}{2}\right) w_2 + (2 - 2\alpha)w_1.$$

We eliminate w_0 from the differential equations (3.4) and obtain

$$\begin{aligned} w_{1tt} &= \frac{1}{h^2}(w_2 - 2w_1 + w_0) = \frac{1}{h^2} \left(\left(1 + \frac{\alpha - \frac{1}{2}}{\frac{3}{2} - \alpha}\right) w_2 - \left(2 - \frac{2 - 2\alpha}{\frac{3}{2} - \alpha}\right) w_1 \right) \\ &= \frac{1}{ah^2}(w_2 - w_1), \quad a = \frac{3}{2} - \alpha. \end{aligned}$$

Thus, (3.4) can be written as

$$(3.7) \quad B\mathbf{w}_{tt} =: \begin{pmatrix} a & & & & & & 0 \\ & 1 & & & & & \\ & & \ddots & & & & \\ & & & \ddots & & & \\ 0 & & & & & & 1 \end{pmatrix} \mathbf{w}_{tt} = \frac{1}{h^2} \begin{pmatrix} -1 & 1 & 0 & 0 & \cdots & 0 \\ 1 & -2 & 1 & 0 & \cdots & \\ 0 & 1 & -2 & 1 & & \\ \vdots & & \ddots & \ddots & \ddots & \\ 0 & & & & & \end{pmatrix} \mathbf{w} := A\mathbf{w}.$$

The matrix A is symmetric and negative definite on the space of grid functions with bounded discrete l_2 -norm. In this way we exclude solutions which are constant in x .

Note that $1/2 \leq a \leq 3/2$, so the system does not become stiff for $0 \leq \alpha \leq 1$. We can therefore apply the scheme (2.8) to integrate in time.

3.2. Higher order methods. It is well known that for the Cauchy problem fourth order methods are much more effective than second order methods when solving wave propagation problems. The number of points/wavelength analysis tells us that the phase error is very much decreased. However, for problems in bounded domains, it is often difficult to construct stable fourth order accurate approximations of the boundary conditions. We want to show that a method that is fourth order accurate in the interior but only second order accurate at the boundary is an acceptable compromise. In this way we control the phase error.

We consider the half-plane problem for the wave equation

$$(3.8) \quad u_{tt} = u_{xx} + F(x, t), \quad x \geq \alpha h, \quad t \geq 0,$$

$$(3.9) \quad u(x, 0) = f^{(1)}(x), \quad u_t(x, 0) = f^{(2)}(x),$$

with Dirichlet boundary conditions

$$(3.10) \quad u(\alpha h, t) = g(t).$$

We approximate (3.8)–(3.10) by

$$(3.11) \quad v_{\nu tt} = D_+ D_- v_{\nu}, \quad v_{\nu} = v(x_{\nu}, t), \quad x_{\nu} = \nu h, \quad \nu = 0, 1, 2, \dots,$$

$$(3.12) \quad v_{\nu}(0) = f_{\nu}^{(1)}, \quad v_{\nu t}(0) = f_{\nu}^{(2)},$$

with boundary condition

$$(3.13) \quad \alpha v_0 + (1 - \alpha)v_1 = g(t).$$

Here $F, f^{(j)}, g \in C_0^\infty$. Without restriction we can assume that $F \equiv 0, f^{(j)} \equiv 0$, because we can extend $F, f^{(j)}$ to the whole space, solve the Cauchy problem, and subtract its solution from u . For the Cauchy problem we know that the fourth order method is much more accurate.

Under the above assumption, we solve the above problems by Laplace transform. The transformed problems are

$$(3.14) \quad s^2 \hat{u} = \hat{u}_{xx}, \quad \hat{u}(\alpha h, s) = \hat{g}, \quad s = i\xi + \eta, \quad \eta > 0,$$

$$(3.15) \quad s^2 \hat{v}_\nu = D_+ D_- \hat{v}_\nu, \quad \alpha v_1 + (1 - \alpha)v_0 = \hat{g}, \quad \nu = 1, 2, \dots,$$

and their solutions are given by

$$(3.16) \quad \hat{u}(x, t) = e^{-sx} e^{\alpha h s} \hat{g},$$

$$(3.17) \quad \hat{v}_\nu = \kappa^\nu \hat{v}_0, \quad (\alpha \kappa + (1 - \alpha)) \hat{v}_0 = \hat{g},$$

respectively. Here κ with $|\kappa| < 1$ is the solution of the characteristic equation

$$\frac{(\kappa - 1)^2}{\kappa} = s^2 h^2.$$

For the discussion of accuracy, we can assume that $|sh| \leq \delta \ll 1$. We obtain

$$\begin{aligned} \kappa &= 1 + \frac{s^2 h^2}{2} - \sqrt{s^2 h^2 + \frac{s^4 h^4}{4}} \sim 1 - sh + \frac{s^2 h^2}{2} - \frac{s^3 h^3}{8} \\ &\sim e^{-sh(1 - \frac{s^2 h^2}{24})}. \end{aligned}$$

By (3.15)

$$v_0 = \frac{\hat{g}}{\alpha e^{-sh} + 1 - \alpha} \sim \hat{g} e^{\alpha h s} \left(1 - \frac{\alpha - \alpha^2}{2} s^2 h^2 \right).$$

Thus, for $x = x_\nu$,

$$\hat{v}(x, s) \sim e^{-sx(1 - \frac{s^2 h^2}{24})} e^{\alpha h s} \hat{g} \left(1 - \frac{\alpha - \alpha^2}{2} s^2 h^2 \right)$$

and

$$(3.18) \quad |\hat{u}(x, s) - \hat{v}(x, s)| \leq |\hat{g} e^{\alpha h s}| \left\{ \left| \frac{\alpha - \alpha^2}{2} s^2 h^2 \right| + |e^{-sx}| \left(1 - e^{\frac{sxh^2 s^2}{24}} \right) \right\}$$

$$(3.19) \quad \sim |\hat{g}| \left(\frac{|sh|^2}{8} + \frac{|sx|}{24} |sh|^2 \right) = \frac{|\hat{g}| |sh|^2}{8} \left(1 + \frac{|sx|}{3} \right).$$

We can invert the Laplace transform on the imaginary axis $s = i\xi$. Therefore, we can consider $u(x, t), v(x, t)$ as a superposition of waves which travel into the region. The error consists of the phase error $\frac{|sx|}{24} (sh)^2$ and the boundary error $\frac{|sh|^2}{8}$, due to the interpolation on the boundary. It shows that the phase error dominates the boundary error if $|sx| > 3$.

We now consider the fourth order method

$$(3.20) \quad v_{\nu tt} = D_+ D_- v_\nu - \frac{h^2}{12} D_+^2 D_-^2 v_\nu, \quad \nu = 1, 2, \dots,$$

with boundary condition

$$(3.21) \quad \alpha v_1 + (1 - \alpha)v_0 = g.$$

Now the stencil depends also on v_{-1} . Therefore, we have to supply an extra boundary such that we can eliminate v_{-1} . This condition can have different forms, depending on our requirements.

3.2.1. A method that is fourth order accurate in the interior and on the boundary. Using the differential equation, the boundary condition

$$u(x, 0) = g(t)$$

implies

$$u_{xx}(x, 0) = u_{tt}(x, 0) = g_{tt}.$$

Therefore, we obtain a method that is fourth order accurate overall if we add the condition

$$(3.22) \quad \alpha D_+ D_- v_1 + (1 - \alpha) D_+ D_- v_0 = g_{tt}.$$

Another advantage of (3.22) is that in matrix form we obtain a symmetric system. We write (3.20) and (3.21), (3.22) in the form

$$\begin{aligned} v_{\nu tt} &= D_+ D_- v_\nu - \frac{h^2}{12} D_+ D_- w_\nu, \quad w_\nu = D_+ D_- v_\nu, \quad \nu = 0, 1, 2, \dots, \\ \alpha v_1 + (1 - \alpha)v_0 &= g, \quad \alpha w_1 + (1 - \alpha)w_0 = g. \end{aligned}$$

Then we can eliminate v_0 and w_0 and obtain

$$\mathbf{v}_{tt} = A\mathbf{v} - \frac{h^2}{12} A\mathbf{w} + F = A\mathbf{v} - \frac{h^2}{12} A^2\mathbf{v} + F.$$

Since $A - \frac{h^2}{12} A^2$ is negative definite, we can apply our previous results and obtain a stable scheme. Unfortunately, this technique cannot easily be generalized to more space dimensions.

3.2.2. Methods that are fourth order accurate in the interior but only second order accurate on the boundary. As we have seen earlier, the error at the boundary is often much smaller than the phase error in the interior. Therefore, it is reasonable to use a method that is fourth order accurate in the interior and second order accurate at the boundary.

The simplest way to achieve this is to calculate the fourth order term only if its stencil does not depend on boundary or exterior points. The resulting scheme is not symmetric and, unfortunately, it is slightly unstable.

We can also replace (3.20) by

$$(3.23) \quad v_{\nu tt} = D_+ D_- v_\nu - \frac{h^2}{12} D_+ D_- (\gamma_\nu D_+ D_- v_\nu), \quad \nu = 1, 2, \dots,$$

with $\gamma_0 = \gamma_1 = 0, \gamma_2 = \gamma_3 = \dots = 1$. Since

$$(3.24) \quad h^2 D_+ D_- (\gamma_\nu D_+ D_- v_\nu) = \gamma_{\nu+1} D_+ D_- v_{\nu+1} - 2\gamma_\nu D_+ D_- v_\nu + \gamma_{\nu-1} D_+ D_- v_{\nu-1},$$

the matrix for the semidiscrete problem is again symmetric and negative definite and we obtain an energy estimate. We shall now discuss the accuracy of the new method. Since the fourth order terms do not depend on v_{-1} and v_0 , we do not need to specify an extra boundary condition. Thus, we consider (3.23) with boundary condition (3.21) and solve the problem by Laplace transform.

Since $\gamma_\nu = 1$ for $\nu \geq 2$, the Laplace transformed problem becomes, using (3.24),

$$(3.25) \quad s^2 \hat{v}_\nu = D_+ D_- \hat{v}_\nu - \frac{h^2}{12} D_+^2 D_-^2 \hat{v}_\nu, \quad \operatorname{Re}(s) > 0, \quad \nu = 3, 4, \dots,$$

$$(3.26) \quad s^2 \hat{v}_2 = D_+ D_- \hat{v}_2 - \frac{1}{12} D_+ D_- \hat{v}_3 + \frac{1}{6} D_+ D_- \hat{v}_2,$$

$$(3.27) \quad s^2 \hat{v}_1 = D_+ D_- \hat{v}_1 - \frac{1}{12} D_+ D_- \hat{v}_2,$$

$$(3.28) \quad \alpha \hat{v}_1 + (1 - \alpha) \hat{v}_0 = \hat{g}.$$

We can eliminate \hat{v}_0 by writing (3.27) and (3.28) in the form

$$(3.29) \quad -(1 - \alpha) \left(h^2 s^2 \hat{v}_1 - h^2 D_+ D_- \hat{v}_1 + \frac{h^2}{12} D_+ D_- \hat{v}_2 \right) = \alpha \hat{v}_1 + (1 - \alpha) \hat{v}_0 - \hat{g}.$$

We now solve (3.25), (3.26), and (3.29). The general solution of (3.25) is

$$(3.30) \quad \hat{v}_\nu = \sigma_1 \kappa_1^\nu + \sigma_2 \kappa_2^\nu,$$

where κ with $|\kappa| < 1$ are solutions of

$$s^2 h^2 = \mu - \frac{1}{12} \mu^2, \quad \mu = \frac{(\kappa - 1)^2}{\kappa}.$$

For small $|sh|$, the solutions of

$$\mu^2 - 12\mu + 12s^2 h^2 = 0$$

are

$$\begin{aligned} \mu_1 &= 6 + \sqrt{36 - 12s^2 h^2} \sim 12, \\ \mu_2 &= 6 - \sqrt{36 - 12s^2 h^2} \\ &= 6 \left(1 - \sqrt{1 - \frac{1}{3} s^2 h^2} \right) \\ &\sim 6 \left(1 - \left(1 - \frac{1}{6} s^2 h^2 - \frac{1}{72} s^4 h^4 - \frac{1}{3^3 \cdot 16} s^6 h^6 \right) \right) \\ &\sim s^2 h^2 + \frac{1}{12} s^4 h^4 + \frac{1}{72} s^6 h^6. \end{aligned}$$

The corresponding κ are solutions of

$$\kappa^2 - (2 + \mu)\kappa + 1 = 0.$$

After some painful computations,

$$(3.31) \quad \kappa_1 \sim \frac{1}{12},$$

$$(3.32) \quad \kappa_2 = 1 + \frac{\mu_2}{2} - \sqrt{\mu_2 + \frac{\mu_2^2}{4}} \sim e^{-sh(1+\gamma(sh)^4)}, \quad \gamma \sim \frac{1}{120}.$$

Inserting the ansatz (3.30) into (3.26),

$$\begin{aligned} &\sigma_1 \kappa_1^2 \left(s^2 h^2 - \frac{7(\kappa_1 - 1)^2}{6\kappa_1} + \frac{1}{12}(\kappa_1 - 1)^2 \right) \\ &+ \sigma_2 \kappa_2^2 \left(s^2 h^2 - \frac{7(\kappa_2 - 1)^2}{6\kappa_2} + \frac{1}{12}(\kappa_2 - 1)^2 \right) = 0, \end{aligned}$$

and entering the above values of κ_1 and κ_2 yields

$$(3.33) \quad \frac{\sigma_1}{12^2} \left(\frac{11^2}{12^2} \left(-14 + \frac{1}{12} \right) + s^2 h^2 \right) - \sigma_2 \left(\frac{s^2 h^2}{12} + O((sh)^3) \right) = 0.$$

Thus we can neglect σ_1 in (3.29) and commit an error $O(h^2 s^2)$ if we replace (3.29) by (3.28). The result is a solution with essentially the same amplitude as in the second order case but with a much improved phase error.

Similar arguments can be used for Neumann boundary conditions. In one space dimension we can obtain an approximation which is fourth order overall by using

$$u_x = g, \quad u_{xtt} = u_{xxx} = g_{tt},$$

as boundary conditions. That the approximation is second order accurate for Dirichlet conditions at the boundary depends crucially on the relation (3.33), which holds only because the boundary condition (3.28) has no influence on (3.26). Second order accurate discrete Neumann conditions depend on v_0, v_1 , and v_2 . Therefore, we will obtain (3.33) only if we replace (3.23) by

$$(3.34) \quad \gamma_0 = \gamma_1 = \gamma_2 = 0, \quad \gamma_\nu = 1 \quad \text{for } \nu \geq 3.$$

In one space dimension this new approximation is stable. We will investigate the two-dimensional Neumann problem in a forthcoming paper.

4. The wave equation in two space dimensions with Dirichlet boundary condition. In this section we consider the scalar wave equation in the bounded domain $\Omega \subset \mathbb{R}^2$, subject to Dirichlet conditions on the boundary Γ ,

$$(4.1) \quad \begin{aligned} u_{tt} &= \Delta u, \quad \mathbf{x} \in \Omega, \quad t > 0, \\ u(\mathbf{x}, t) &= f(\mathbf{x}, t), \quad \mathbf{x} \in \Gamma, \quad t > 0, \\ u(\mathbf{x}, 0) &= u_0(\mathbf{x}), \quad u_t(\mathbf{x}, 0) = u_1(\mathbf{x}), \quad \mathbf{x} \in \Omega. \end{aligned}$$

4.1. Algorithm. We cover Ω by a Cartesian grid with step size h ; see Figure 1. The grid points are given by $\mathbf{x}_{i,j} = (x_i, y_j)^T$,

$$\begin{aligned} x_i &= x^{(0)} + (i - 1)h, \quad i = 1, 2, \dots, N, \\ y_j &= y^{(0)} + (j - 1)h, \quad j = 1, 2, \dots, M, \end{aligned}$$

where $h = (x^{(1)} - x^{(0)}) / (N - 1) \equiv (y^{(1)} - y^{(0)}) / (M - 1)$. Let all points $\mathbf{x} = (x, y) \in \Omega$ satisfy $x_{\min} \leq x \leq x_{\max}$, $y_{\min} \leq y \leq y_{\max}$. To make sure the grid covers Ω , we require $x^{(0)} \leq x_{\min} - h$, $x^{(1)} \geq x_{\max} + h$ and $y^{(0)} \leq y_{\min} - h$, $y^{(1)} \geq y_{\max} + h$.

Before we can discretize the problem, we need to classify each grid point. We denote the classification by $m_{i,j}$,

$$m_{i,j} = \begin{cases} 0, & \mathbf{x}_{i,j} \text{ outside of } \Omega, \\ 1, & \mathbf{x}_{i,j} \in \Omega, \mathbf{x}_{i\pm 1,j} \in \Omega \text{ and } \mathbf{x}_{i,j\pm 1} \in \Omega, \\ -1 & \text{otherwise.} \end{cases}$$

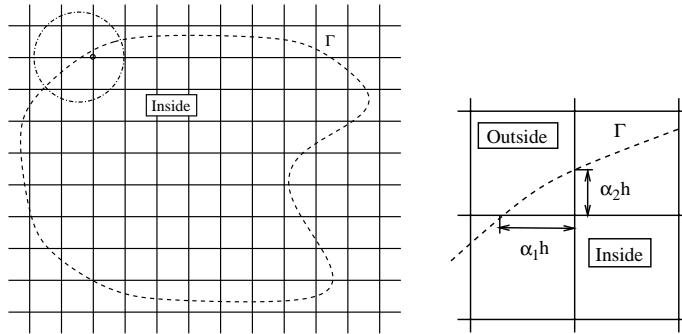


FIG. 1. The computational grid and the embedded boundary (left) and a close-up of one boundary point (right).

Hence, interior points have $m_{i,j} = 1$, exterior points have $m_{i,j} = 0$, and boundary points have $m_{i,j} = -1$. Let $u_{i,j}^n$ denote the difference approximation to $u(x_i, y_j, t_n)$. At interior points, we use a centered approximation both in space and time,

$$(4.2) \quad \frac{u_{i,j}^{n+1} - 2u_{i,j}^n + u_{i,j}^{n-1}}{k^2} = (D_+^x D_-^x + D_+^y D_-^y)u_{i,j}^n =: \Delta_h u_{i,j}^n, \quad m_{i,j} = 1.$$

At boundary points, the Dirichlet boundary condition is used to eliminate the exterior points from the centered difference formula. For example, let $\mathbf{x}_{i,j}$ be a boundary point and let the points $(x_i - \alpha_1 h, y_j)^T$ and $(x_i, y_j + \alpha_2 h)^T$ be on the boundary, as is shown in Figure 1. The Dirichlet conditions are approximated by linear interpolation,

$$\begin{aligned} (1 - \alpha_1)u_{i,j}^n + \alpha_1 u_{i-1,j}^n &= f(x_i - \alpha_1 h, y_j, t_n), \\ (1 - \alpha_2)u_{i,j}^n + \alpha_2 u_{i,j+1}^n &= f(x_i, y_j + \alpha_2 h, t_n). \end{aligned}$$

Assuming that $\alpha_1 > 0, \alpha_2 > 0$,

$$\begin{aligned} u_{i-1,j}^n &= -\frac{1 - \alpha_1}{\alpha_1} u_{i,j}^n + \frac{1}{\alpha_1} f(x_i - \alpha_1 h, y_j, t_n), \\ u_{i,j+1}^n &= -\frac{1 - \alpha_2}{\alpha_2} u_{i,j}^n + \frac{1}{\alpha_2} f(x_i, y_j + \alpha_2 h, t_n). \end{aligned}$$

Eliminating $u_{i-1,j}^n$ and $u_{i,j+1}^n$ from (4.2) results in

$$(4.3) \quad \frac{u_{i,j}^{n+1} - 2u_{i,j}^n + u_{i,j}^{n-1}}{k^2} = \frac{1}{h^2} (-(4 + d_{i,j})u_{i,j}^n + u_{i+1,j}^n + u_{i,j-1}^n) + \frac{\tilde{f}_{i,j}^n}{h^2}$$

$$(4.4) \quad =: \tilde{\Delta}_h u_{i,j}^n + \frac{\tilde{f}_{i,j}^n}{h^2},$$

where $d_{i,j} = (1 - \alpha_1)/\alpha_1 + (1 - \alpha_2)/\alpha_2 > 0$ and $\tilde{f}_{i,j}^n = f(x_i - \alpha_1 h, y_j, t_n)/\alpha_1 + f(x_i, y_j + \alpha_2 h, t_n)/\alpha_2$. Since α_1 and α_2 can be arbitrarily close to zero, d can be very large, which makes the time-step restriction for (4.4) severe. To avoid this problem, we use the splitting discussed in section 2,

$$\begin{aligned} \frac{u_{i,j}^{n+1} - 2u_{i,j}^n + u_{i,j}^{n-1}}{k^2} &= \frac{1}{h^2} (-4u_{i,j}^n + u_{i+1,j}^n + u_{i,j-1}^n) \\ &\quad - \frac{d_{i,j}}{2h^2} (u_{i,j}^{n+1} + u_{i,j}^{n-1}) + \frac{\tilde{f}_{i,j}^n}{h^2}, \quad m_{i,j} = -1. \end{aligned}$$

In the general case, $d_{i,j}$ and $\tilde{f}_{i,j}^n$ get contributions from all exterior nearest neighbors, and the first term on the right-hand side includes all interior or boundary nearest neighbors,

$$(4.5) \quad \frac{u_{i,j}^{n+1} - 2u_{i,j}^n + u_{i,j}^{n-1}}{k^2} = \frac{1}{h^2} \left(-4u_{i,j}^n + \sum_{\mathbf{j}} |m_{\mathbf{j}}| u_{\mathbf{j}}^n \right) - \frac{d_{i,j}}{2h^2} (u_{i,j}^{n+1} + u_{i,j}^{n-1}) + \frac{\tilde{f}_{i,j}^n}{h^2}, \quad m_{i,j} = -1.$$

Here \mathbf{j} is a multi-index and the sum extends over all nearest neighbors $\mathbf{j} = (i + 1, j), (i - 1, j), (i, j + 1), (i, j - 1)$.

4.2. Stability. By letting \mathbf{u}^n denote the vector containing the solution $u_{i,j}^n$ at all interior and boundary points (using line ordering, for example), we can write the time-integration scheme (4.2), (4.5) in the form (2.11). The matrix A_1 , given by

$$A_1 \mathbf{u} = \begin{cases} 0, & m_{i,j} = 1, \\ -\frac{d_{i,j}}{h^2}, & m_{i,j} = -1, \end{cases}$$

is negative semidefinite since it is diagonal and $-d_{i,j} < 0$. The matrix A_2 is defined by

$$A_2 \mathbf{u} = \begin{cases} \frac{1}{h^2} \left(-4u_{i,j} + \sum_{\mathbf{j}} u_{\mathbf{j}} \right), & m_{i,j} = 1, \\ \frac{1}{h^2} \left(-4u_{i,j} + \sum_{\mathbf{j}} |m_{\mathbf{j}}| u_{\mathbf{j}} \right), & m_{i,j} = -1. \end{cases}$$

Again, the sum extends over all nearest neighbors $\mathbf{j} = (i + 1, j), (i - 1, j), (i, j + 1), (i, j - 1)$.

To study the symmetry of A_2 , we note that if (i, j) is an interior point, the corresponding row in $A_2 \mathbf{u}$ contains the four off-diagonal terms $u_{i+1,j} + u_{i-1,j} + u_{i,j+1} + u_{i,j-1}$. On the other hand, the row in $A_2 \mathbf{u}$ corresponding to point $(i + 1, j)$ includes the term $u_{i,j}$, whether $(i + 1, j)$ is an interior or a boundary point. The same argument applies to the other three off-diagonal terms. When (i, j) is a boundary point, the corresponding row in $A_2 \mathbf{u}$ contains at most three off-diagonal terms. For example, let one of these terms be $u_{i+1,j}$. Again, the row in $A_2 \mathbf{u}$ corresponding to point $(i + 1, j)$ includes the term $u_{i,j}$. We conclude that the matrix A_2 is symmetric.

Since the sum of all elements on each row of A_2 is less than or equal to zero, the Gershgorin circle theorem implies that A_2 is negative semidefinite. We proceed by showing that A_2 is negative definite. We begin with the case when Γ is convex; see Figure 2. Let us define the inner product between two real-valued grid functions \mathbf{u} and \mathbf{v} by

$$(\mathbf{u}, \mathbf{v})_h = \sum_{i=1}^N \sum_{j=js(i)}^{je(i)} u_{i,j} v_{i,j} \equiv \sum_{j=1}^M \sum_{i=is(j)}^{ie(j)} u_{i,j} v_{i,j}.$$

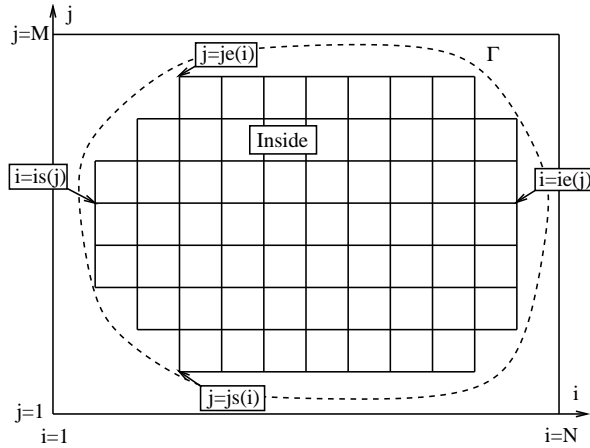


FIG. 2. Notation used to show that A_2 is negative definite.

It is convenient to treat the terms in $(\mathbf{u}, A_2 \mathbf{u})_h$ “dimension by dimension.” We have

$$\begin{aligned}
 (\mathbf{u}, A_2 \mathbf{u})_h &= \sum_{i=1}^N S_1(i) + \sum_{j=1}^M S_2(j), \\
 S_1(i) &= \sum_{j=js(i)+1}^{je(i)-1} u_{i,j} D_+^y D_-^y u_{i,j} + \frac{1}{h^2} u_{i,js(i)} (-2u_{i,js(i)} + u_{i,js(i)+1}) \\
 &\quad + \frac{1}{h^2} u_{i,je(i)} (-2u_{i,je(i)} + u_{i,je(i)-1}), \\
 S_2(j) &= \sum_{i=is(j)+1}^{ie(j)-1} u_{i,j} D_+^x D_-^x u_{i,j} + \frac{1}{h^2} u_{is(j),j} (-2u_{is(j),j} + u_{is(j)+1,j}) \\
 &\quad + \frac{1}{h^2} u_{ie(j),j} (-2u_{ie(j),j} + u_{ie(j)-1,j}).
 \end{aligned}$$

The sum in $S_1(i)$ satisfies

$$\begin{aligned}
 \sum_{j=js(i)+1}^{je(i)-1} u_{i,j} D_+^y D_-^y u_{i,j} &= \sum_{j=js(i)+1}^{je(i)-1} u_{i,j} \frac{1}{h} (D_-^y u_{i,j+1} - D_-^y u_{i,j}) \\
 &= - \sum_{j=js(i)+1}^{je(i)-1} (D_-^y u_{i,j})^2 - \frac{u_{i,js(i)}}{h} D_-^y u_{i,js(i)+1} + \frac{u_{i,je(i)-1}}{h} D_-^y u_{i,je(i)}.
 \end{aligned}$$

Now, the two last terms in $S_1(i)$ satisfy

$$\begin{aligned}
 &\frac{u_{i,js(i)}}{h^2} (-2u_{i,js(i)} + u_{i,js(i)+1}) + \frac{u_{i,je(i)}}{h^2} (-2u_{i,je(i)} + u_{i,je(i)-1}) \\
 &= -\frac{u_{i,js(i)}^2}{h^2} + \frac{u_{i,js(i)}}{h} D_-^y u_{i,js(i)+1} - \frac{u_{i,je(i)}^2}{h^2} - \frac{u_{i,je(i)}}{h} D_-^y u_{i,je(i)}.
 \end{aligned}$$

Therefore,

$$S_1(i) = - \sum_{j=js(i)+1}^{je(i)} (D_-^y u_{i,j})^2 - \frac{u_{i,js(i)}^2}{h^2} - \frac{u_{i,je(i)}^2}{h^2}.$$

In the same way,

$$S_2(j) = - \sum_{i=is(j)+1}^{ie(j)} (D_-^x u_{i,j})^2 - \frac{u_{is(j),j}^2}{h^2} - \frac{u_{ie(j),j}^2}{h^2}.$$

Since all terms in $(\mathbf{u}, A_2 \mathbf{u})_h$ are less than or equal to zero, $(\mathbf{u}, A_2 \mathbf{u})_h$ can only be zero if all terms are zero. For example, $S_1(i) = 0$ if and only if

$$\begin{aligned} D_-^y u_{i,j} &= 0, & js(i) + 1 \leq j \leq je(i), \\ u_{i,js(i)} &= 0, \\ u_{i,je(i)} &= 0, \end{aligned}$$

which implies $u_{i,j} \equiv 0$, $js(i) \leq j \leq je(i)$. In the same way, $S_2(j) = 0$ if and only if $u_{i,j} \equiv 0$, $is(j) \leq i \leq ie(j)$. This proves that $(\mathbf{u}, A_2 \mathbf{u})_h = 0$ if and only if $\mathbf{u} \equiv 0$. The nonconvex case can be handled in the same way, except that the terms S_1 and S_2 must be divided into several parts, corresponding to the number of times the boundary splits the same grid line. Hence, the matrix A_2 is negative definite for both convex and nonconvex boundaries.

We have shown that both A_1 and A_2 are symmetric, A_1 is negative semidefinite, and A_2 is negative definite. Hence, Lemma 2.2 applies, so the time-step restriction of (4.2), (4.5) is determined only by A_2 , i.e., the interior formula, and the solution is uniformly bounded in time. Moreover, the solution at the new time level, \mathbf{u}^{n+1} , can be computed pointwise since the matrix A_1 is diagonal.

4.3. Accuracy. We have constructed our difference approximation “dimension by dimension.” If we write the approximation in matrix form, the coefficient matrix is symmetric and negative definite. Therefore, there are no stability problems. However, it is not obvious that the approximation is second order accurate. The reason is that an exterior point P can have two interior points P_1, P_2 as neighbors, P_1 in the x -direction and P_2 in the y -direction; see Figure 3. In this case the value of u at P is not unique, since it depends on which interpolation direction we use. For our scheme, this does not matter because we eliminate $u(P)$ both from $D_+^x D_-^x u(P_1)$ and $D_+^y D_-^y u(P_2)$, using the corresponding interpolation formula. However, the usual truncation error analysis fails.

We shall now use a more refined argument to show that the approximation is second order accurate. For simplicity, we study only the semidiscrete problem where time is left continuous,

$$(4.6) \quad \begin{aligned} \frac{\partial^2 u_h}{\partial t^2} &= \tilde{\Delta}_h u_h + \frac{\tilde{f}}{h^2}, \\ u_h(\mathbf{x}_j, 0) &= u_0(\mathbf{x}_j), \quad \frac{\partial u_h}{\partial t}(\mathbf{x}_j, 0) = u_1(\mathbf{x}_j). \end{aligned}$$

We assume that the solution of the continuous wave equation (4.1) is smooth and can be extended smoothly from Ω to a larger region Ω_1 which contains all external points

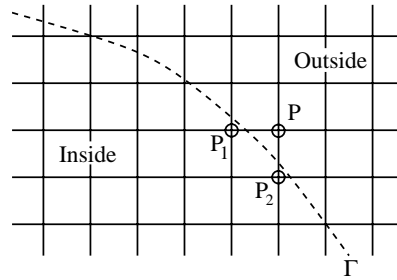


FIG. 3. The outside point P is used when discretizing the Laplacian at both of the inside points P_1 and P_2 .

with boundary points as neighbors. Let $u(x, y, t)$ be the solution of (4.1). It solves the inhomogeneous difference equation

$$(4.7) \quad u_{tt} = \Delta_h u + h^2 G.$$

Here $h^2 G$ represents the truncation error. Let $P_1 = (x, y)$ be a boundary point and $(x + h, y)$ an exterior point. The extended solution satisfies an inhomogeneous interpolation formula:

$$(4.8) \quad (1 - \alpha_1)u(x, y, t) + \alpha_1 u(x + h, y, t) = f(x + \alpha_1 h, y, t) + h^2 g_1.$$

If also $(x, y + h)$ is an exterior point, then there is another interpolation formula:

$$(4.9) \quad (1 - \alpha_2)u(x, y, t) + \alpha_2 u(x, y + h, t) = f(x, y + \alpha_2 h, t) + h^2 g_2.$$

We use (4.8) and (4.9) to eliminate $u(x + h, y, t)$ and $u(x, y + h, t)$ from $D_+^x D_-^x u(x, y, t)$ and $D_+^y D_-^y u(x, y, t)$, respectively. After we have eliminated all exterior points, we obtain

$$(4.10) \quad u_{tt} = \tilde{\Delta}_h u + h^2 G + g + \frac{\tilde{f}}{h^2} \quad \text{for } \mathbf{x} = \mathbf{x}_j, |m_j| = 1, t > 0.$$

Note that $g \neq 0$ and $\tilde{f} \neq 0$ only at boundary points and $\tilde{\Delta}_h u = \Delta_h u$ at all interior points. At boundary points (x, y) (which have at least one neighboring exterior point), we obtain a q -point formula with $q \leq 4$ of the form

$$(4.11) \quad h^2 \tilde{\Delta}_h u(\mathbf{x}_{i,j}, t) = -(4 + d_{i,j})u(\mathbf{x}_{i,j}, t) + \sum_j |m_j| u(\mathbf{x}_j, t),$$

where the sum extends over the nearest neighbors $(x_i \pm h, y_j)$, $(x_i, y_j \pm h)$, and $d_{i,j} > 0$.

Subtracting the difference approximation (4.6) from (4.10) gives us, for the error $e = u - u_h$,

$$e_{tt} = \tilde{\Delta}_h e + h^2 G + g, \\ e(\cdot, 0) = e_t(\cdot, 0) = 0.$$

To analyze the effect the term g has on the error, we study

$$\tilde{\Delta}_h \varphi = g.$$

Away from the boundary, $g = 0$ and $\tilde{\Delta}_h = \Delta_h$. It is easy to show that the solution of

$$\begin{aligned} \Delta_h \phi_{i,j} &= 0, & m_{i,j} &= 1, \\ \phi_{i,j} &= \gamma_{i,j}, & m_{i,j} &= -1, \end{aligned}$$

takes its maximum at a boundary point (where $m_{i,j} = -1$). Let (x_i, y_j) be the boundary point where $|\varphi(x_i, y_j)| = |\varphi|_\infty$. From (4.11) we have

$$(4 + d_{i,j})|\varphi|_\infty \leq \sum_j |m_j| |\varphi|_\infty + h^2 |g|_\infty.$$

Hence,

$$|\varphi|_\infty \leq \frac{h^2}{4 + d_{i,j} - \sum_j |m_j|} |g|_\infty.$$

Since $d_{i,j} > 0$ and $\sum_j |m_j| \leq 3$,

$$|\varphi|_\infty \leq h^2 |g|_\infty.$$

From the definition of g , it is a smooth function of t . Therefore, $\tilde{e} = e + \varphi$ solves

$$\tilde{e}_{tt} = \tilde{\Delta}_h \tilde{e} + h^2 G + \varphi_{tt}, \quad |\varphi_{tt}|_\infty \leq h^2 |g_{tt}|_\infty,$$

i.e.,

$$|e|_\infty = \mathcal{O}(h^2).$$

This shows that the approximation is second order accurate.

5. Numerical examples. In this section we consider (4.1) with a forcing function,

$$(5.1) \quad \begin{aligned} u_{tt} &= \Delta u + F(\mathbf{x}, t), & \mathbf{x} &\in \Omega, \quad t > 0, \\ u(\mathbf{x}, t) &= f(\mathbf{x}, t), & \mathbf{x} &\in \Gamma, \quad t > 0, \\ u(\mathbf{x}, 0) &= u_0(\mathbf{x}), \quad u_t(\mathbf{x}, 0) = u_1(\mathbf{x}), & \mathbf{x} &\in \Omega. \end{aligned}$$

This problem will be solved by both a fully second and an internally fourth order accurate method, and the forcing functions will be chosen such that an exact solution is known. The second order scheme is given by (4.2) and (4.5), and the internally fourth order scheme is obtained by adding the correction term

$$\Delta_{h,4} v_{i,j}^n = -\frac{h^2}{12} (D_+^x D_-^x \gamma_{i,j} D_+^x D_-^x + D_+^y D_-^y \gamma_{i,j} D_+^y D_-^y) v_{i,j}^n$$

to the right-hand sides of (4.2) and (4.5), respectively. Here

$$\gamma_{i,j} = \begin{cases} 1, & m_{i,j} = 1, \\ 0 & \text{otherwise,} \end{cases}$$

where $m_{i,j}$ is defined in section 4.1.

The correction term $\Delta_{h,4} v_{i,j}^n$ gives a symmetric negative semidefinite contribution to the matrix representation of the scheme that does not involve the boundary.

TABLE 1

Grid refinement study for the Dirichlet problem for a trigonometric exact solution; CFL = 0.5.

t	2'nd order error			4'th order error		
	$N = 100$	$N = 200$	ratio	$N = 100$	$N = 200$	ratio
0.330	2.54e-02	5.77e-03	4.4	1.27e-02	3.58e-03	3.5
1.980	2.30e-02	5.47e-03	4.2	1.46e-02	3.97e-03	3.7

Hence, the internally fourth order scheme is stable. However, the internally fourth order scheme can be expected to be only second order accurate near the boundary, since a second order approximation of the Dirichlet boundary condition is used. For simplicity, the internally fourth order scheme will henceforth be called the fourth order scheme.

We start the numerical integration at $n = 0$. For the cases where an analytical solution is known, we use this solution to initialize the computation at time levels t_{-1} and t_0 . For the cases where an analytical solution is not known we use the initialization

$$v_{i,j}^{-1} = u_0(x_i, y_j) - ku_1(x_i, y_j) + \frac{k^2}{2}(D_+^x D_-^x + D_+^y D_-^y)u_0(x_i, y_j),$$

and $v_{i,j}^0 = u_0(x_i, y_j)$.

We will denote the CFL-number by $\text{CFL} \equiv k/h$. Note that for a two-dimensional periodic domain, the scheme (4.2) is stable for $\text{CFL} \leq 1/\sqrt{2}$. Also note that all errors are measured in the max-norm.

5.1. Convergence study for a trigonometric exact solution. Let us choose the forcing function F and boundary data f such that the exact solution is the trigonometric traveling wave

$$(5.2) \quad u(x, y, t) = \sin(\omega(x - t)) \sin(\omega y), \quad \omega = 4\pi.$$

The domain Ω is taken to be an ellipse centered at the origin with semiaxes $x_s = 1$ and $y_s = 0.75$. The Cartesian grid covers the rectangle $-1.1 \leq x \leq 1.1$, $-0.85 \leq y \leq 0.85$. In Table 1, we present a grid refinement study for the two schemes with $\text{CFL} = 0.5$. In Table 2 we present the same study with $\text{CFL} = 0.1$. Note that the error in the second order scheme is not improved by decreasing the CFL number, indicating that the error is dominated by spatial discretization errors. The error for the fourth order scheme is improved somewhat by decreasing the CFL number, implying that temporal discretization errors cannot be neglected when $\text{CFL} = 0.5$. For both CFL-numbers, the error is smaller for the fourth order scheme than for the second order scheme. However, the order of convergence is only around two for the fourth order scheme and $\text{CFL} = 0.1$. In section 3.2 the spatial discretization error is shown to consist of a second order amplitude error arising from the boundary discretization and a fourth order phase error originating from the discretization in the interior. It is therefore likely that the dominant errors for the fourth order scheme and $\text{CFL} = 0.1$ are generated at the boundary.

5.2. Convergence study for an inwards traveling wave solution in a circle. To illustrate the benefits of using a fourth order scheme away from the boundary, we select the forcing function F and boundary data f such that the exact solution

TABLE 2

Grid refinement study for the Dirichlet problem for a trigonometric exact solution; CFL = 0.1.

t	2'nd order error			4'th order error		
	$N = 100$	$N = 200$	ratio	$N = 100$	$N = 200$	ratio
0.330	2.31e-02	5.77e-03	4.0	1.06e-02	2.23e-03	4.8
1.980	2.40e-02	5.92e-03	4.1	7.55e-03	2.16e-03	3.5

TABLE 3

Grid refinement study for the Dirichlet problem for an inwards traveling wave solution. Here, CFL = 0.5.

t	2'nd order error			4'th order error
	$N = 400$	$N = 800$	ratio	$N = 400$
0.315	1.51e-02	3.66e-03	4.12	6.51e-03
0.525	3.29e-02	8.79e-03	3.75	1.15e-02
1.155	8.44e-02	2.67e-02	3.17	3.29e-02
1.365	1.03e-01	3.40e-02	3.03	4.16e-02

(in polar coordinates) is a spatially localized traveling wave,

$$(5.3) \quad u(r, t) = \phi(r + t), \quad \phi(\xi) = \frac{1}{4} \left(1 + \tanh \frac{\xi - \xi_0}{\epsilon} \right) \left(1 - \tanh \frac{\xi - \xi_1}{\epsilon} \right).$$

Note that such waves are exact solutions to the unforced wave equation in one and three space dimensions, but they are not in the two-dimensional case. The domain Ω is taken to be the circle, $|r| \leq 2$, and the Cartesian grid covers the square $-2.1 \leq x \leq 2.1$, $-2.1 \leq y \leq 2.1$.

The parameters in the exact solution are chosen so that initially the wave is essentially outside the domain and enters the region through the boundary after some time. To make the problem challenging to solve numerically, we make the transitions around $\xi = \xi_0$ and $\xi = \xi_1$ rapid and close together by choosing

$$\xi_0 = 2.2, \quad \xi_1 = 2.4, \quad \epsilon = 0.035.$$

The maximum of the wave reaches the boundary at $t = 0.3$ and has passed through the boundary after $t \approx 0.4 - 0.5$. In Table 3 we present a study of the errors for the two schemes with CFL=0.5 both when the wave has reached the boundary and after the wave has passed the boundary. In Table 4 we present a similar study but with CFL= 0.1. Note first that the error in the fourth order scheme is improved by decreasing the CFL-number for $N = 400$, indicating again that time discretization errors are not small when CFL= 0.5. Furthermore, note that the fourth order method with CFL= 0.1 gives close to fourth order accuracy after the wave has passed the boundary, implying that the phase error dominates; see the discussions in sections 5.1 and 3.2. Also, the error in the second order scheme does not improve when the CFL number is decreased, indicating again that the second order scheme is dominated by spatial discretization errors. When 400 grid points are used in each direction, the second order scheme produces a solution that has many spurious oscillations, while the fourth order scheme gives a much cleaner result; see Figure 4.

TABLE 4

Grid refinement study for the Dirichlet problem for an inwards traveling wave solution. Here, CFL = 0.1.

t	2'nd order error	4'th order error		
	$N = 400$	$N = 400$	$N = 800$	ratio
0.315	1.73e-02	4.39e-03	8.37e-04	5.24
0.525	3.98e-02	6.55e-03	8.30e-04	7.89
1.155	9.95e-02	1.09e-02	8.12e-04	13.44
1.365	1.20e-01	1.31e-02	9.64e-04	13.62

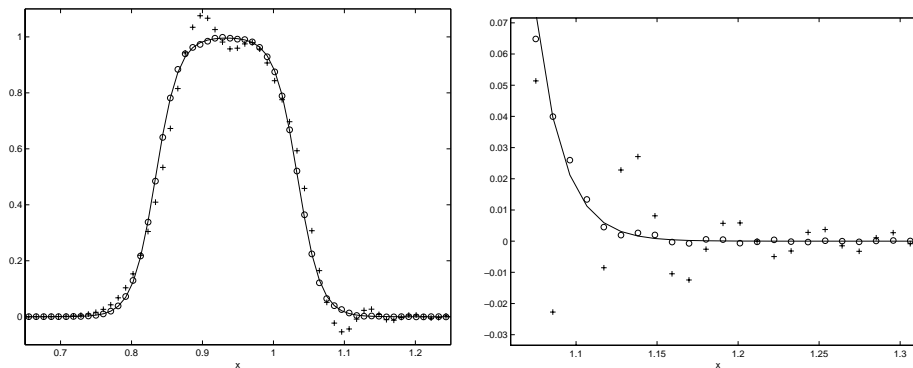


FIG. 4. The inwards traveling wave solution for the Dirichlet problem along the line $y = -h/2$ at time $t = 1.365$. The right figure shows a close-up centered around $x = 1.2$. The exact solution is a solid line, the computed solution with the second order scheme is denoted by (+), and the fourth order scheme is marked with (o). In these computations, $N = 400$ and CFL = 0.1.

5.3. Convergence study for an outwards traveling wave solution in a circle. To further study the benefits of using a fourth order scheme away from the boundary, we let the exact solution be an outwards traveling wave,

$$(5.4) \quad u(r, t) = \phi(r - t),$$

where ϕ is given by (5.3). The domain Ω is in this case taken to be the unit circle, $|r| \leq 1$, and the Cartesian grid covers the square $-1.1 \leq x \leq 1.1$, $-1.1 \leq y \leq 1.1$. Here, the parameters in ϕ are taken to be

$$\xi_0 = 0.2, \quad \xi_1 = 0.4, \quad \epsilon = 0.035.$$

The wave reaches the boundary at $t \approx 0.5 - 0.6$ and has passed through the boundary after $t \approx 0.8 - 0.9$. In Table 5 we present a grid convergence study for the two schemes with CFL=0.5 before and after the wave has passed the boundary. In Table 6 we present the same study but with CFL=0.1. Note that the fourth order method gives fourth order convergence for the smaller CFL-number before the wave reaches the boundary and gives second order convergence after the wave has reached the boundary. When 200 grid points are used in each direction, the second order scheme produces a solution that has many spurious oscillations, while the fourth order scheme gives a much cleaner result; see Figure 5.

TABLE 5

Grid refinement study for the Dirichlet problem for an outwards traveling wave solution; CFL = 0.5.

t	2'nd order error			4'th order error		
	$N = 200$	$N = 400$	ratio	$N = 200$	$N = 400$	ratio
0.22	1.99e-02	5.44e-03	3.7	6.70e-03	1.79e-03	3.7
0.33	2.78e-02	7.82e-03	3.6	9.64e-03	2.60e-03	3.7
0.66	5.35e-02	1.40e-02	3.8	1.61e-02	4.47e-03	3.6
0.77	5.77e-02	1.76e-02	3.3	2.30e-02	6.11e-03	3.8

TABLE 6

Grid refinement study for the Dirichlet problem for an outwards traveling wave solution; CFL = 0.1.

t	2'nd order error			4'th order error		
	$N = 200$	$N = 400$	ratio	$N = 200$	$N = 400$	ratio
0.22	2.53e-02	7.08e-03	3.6	2.37e-03	1.40e-04	17.0
0.33	3.50e-02	1.01e-02	3.5	3.33e-03	2.03e-04	16.5
0.66	5.73e-02	1.71e-02	3.3	8.50e-03	7.34e-04	11.6
0.77	6.46e-02	2.23e-02	2.9	8.26e-03	1.17e-03	7.1

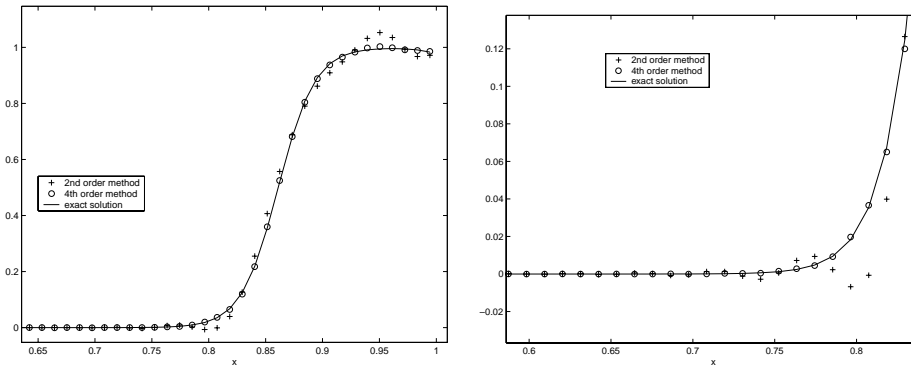


FIG. 5. The outwards traveling wave solution for the Dirichlet problem along the line $y = -h/2$ at time $t = 0.66$. The right figure shows a close-up centered around $x = 0.7$. The exact solution is a solid line, the computed solution with the second order scheme is denoted by (+), and the fourth order scheme is marked with (o). Here $N = 200$ and CFL= 0.1.

5.4. Bouncing wave in an ellipse. Here we study the homogeneous problem

$$F(\mathbf{x}, t) \equiv 0, \quad f(\mathbf{x}, t) \equiv 0,$$

in a domain bounded by an ellipse centered at the origin, with semiaxes $x_s = 2.0$ and $y_s = 2.54$. The Cartesian grid covers the square $-2.1 \leq x \leq 2.1, -2.64 \leq y \leq 2.64$. We take initial data to be

$$u_0(x, y) = \phi(r),$$

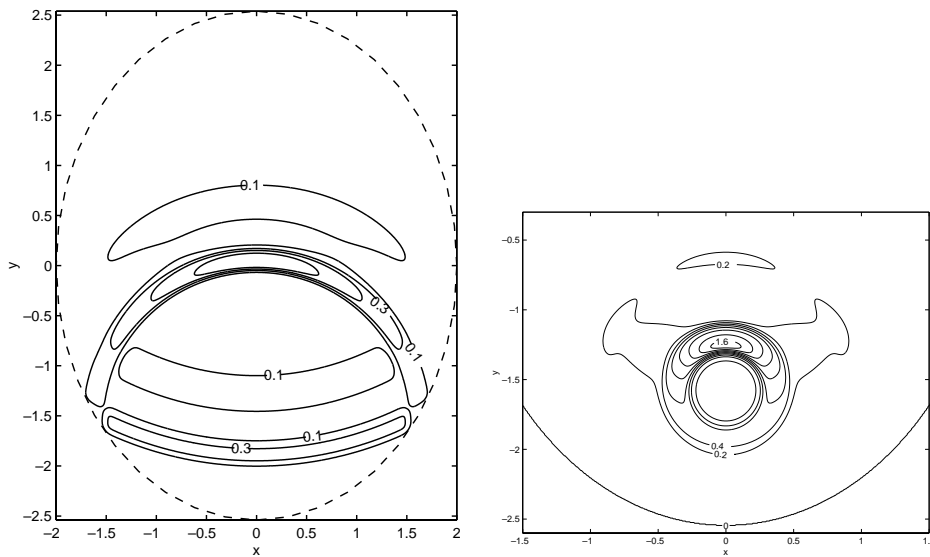


FIG. 6. The bouncing wave reference solution for the Dirichlet problem with the fourth order scheme at $t = 3.15$ (left) and $t = 4.41$ (right). Here $N = 800$, $\text{CFL} = 0.1$. The contour spacing is 0.2, and the dashed curve in the left plot indicates the boundary.

where $\phi(r)$ is given by (5.3) and $r = \sqrt{x^2 + (y - y_F)^2}$. The upper focal point is located at $y_F = \sqrt{y_s^2 - x_s^2} \approx 1.56$ and

$$u_1(\mathbf{x}) = u_1(r) = -\phi'(r).$$

The parameters in $\phi(r)$ are

$$\xi_0 = 0.2, \quad \xi_1 = 0.4, \quad \epsilon = 0.035.$$

Note that the initial data is chosen such that the wave is essentially traveling in the positive r -direction out from the focal point $(0, y_F)$. By making a ray-tracing argument, we see that a high frequency wave should reflect the boundary and refocus at the other focal point $(0, -y_F)$. To verify this behavior, we make a reference calculation using a fine grid with $N = 800$ and the fourth order method with $\text{CFL} = 0.1$. We then make calculations with $N = 400$ and $N = 100$ for the fourth and the second order methods. These solutions are compared to the reference calculation at the time $t = 4.41$, just before the solution is refocused at the other focal point. In Figure 6, we show contour plots of the reference calculation at $t = 3.15$ and $t = 4.41$. In Figure 7, we display contour plots of the solutions using the fourth and second order schemes for $N = 400$ at $t = 4.41$. We also plot the numerical solutions along the line $x = 0$, where the deviation from the reference solution is the largest; see Figure 8. In Figures 9 and 10, the corresponding calculations are presented for $N = 100$. Clearly, the fourth order method gives the best result.

6. Conclusions. Numerical methods have been proposed and analyzed for solving a second order wave equation without first writing it as a first order system. Both the Dirichlet and the Neumann problems were treated for the one-dimensional case. The Dirichlet problem was analyzed in detail for general two-dimensional domains, and we proved that the proposed scheme is stable and conservative both for second and

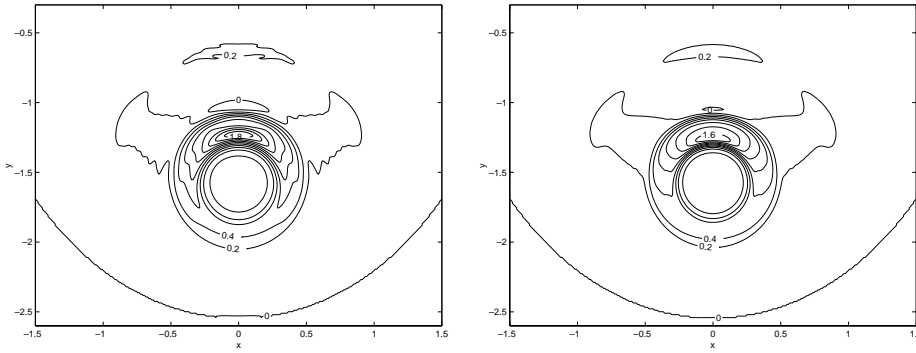


FIG. 7. The bouncing wave solutions for the Dirichlet problem at $t = 4.41$. Left: the second order scheme with $CFL = 0.5, N = 400$. Right: the fourth order scheme with $CFL = 0.1, N = 400$. The contour spacing is 0.2 .

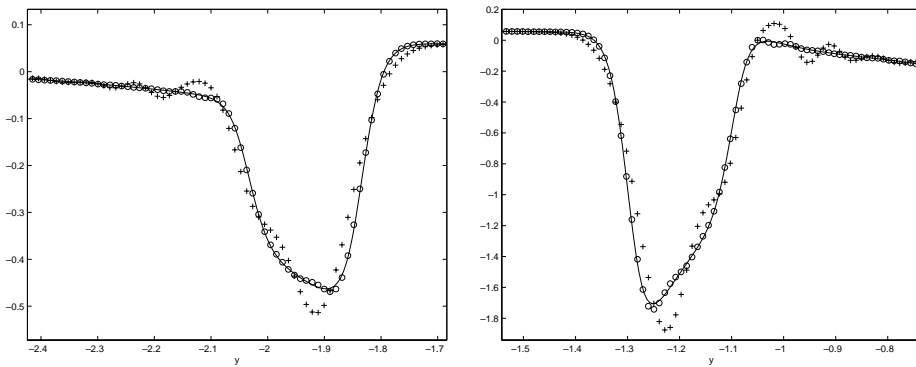


FIG. 8. The bouncing wave solutions on a fine grid for the Dirichlet problem along the line $x = 0$ at $t = 4.41$, centered around $y = -2$ (left) and $y = -1.2$ (right). Solid: the reference solution, “+”: the second order scheme with $CFL = 0.5, N = 400$. “o”: the fourth order scheme with $CFL = 0.1, N = 400$. Note the over- and undershoots obtained with the second order scheme.

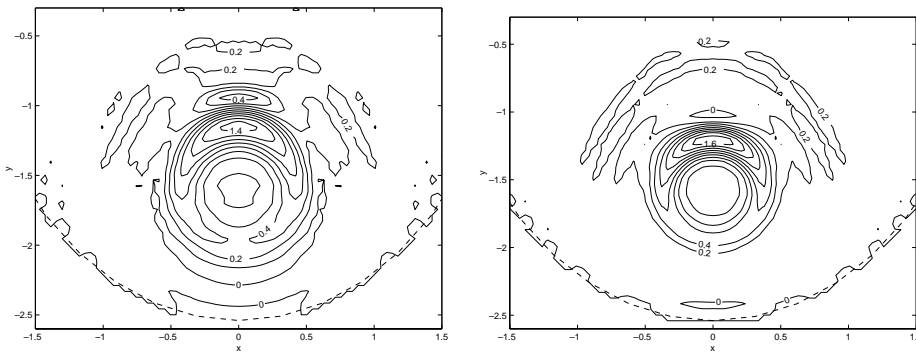


FIG. 9. The bouncing wave solutions on a coarse grid for the Dirichlet problem at $t = 4.41$. Left: the second order scheme with $CFL = 0.5, N = 100$. Right: the fourth order scheme with $CFL = 0.1, N = 100$. The contour spacing is 0.2 , and the dashed curve represents the boundary.

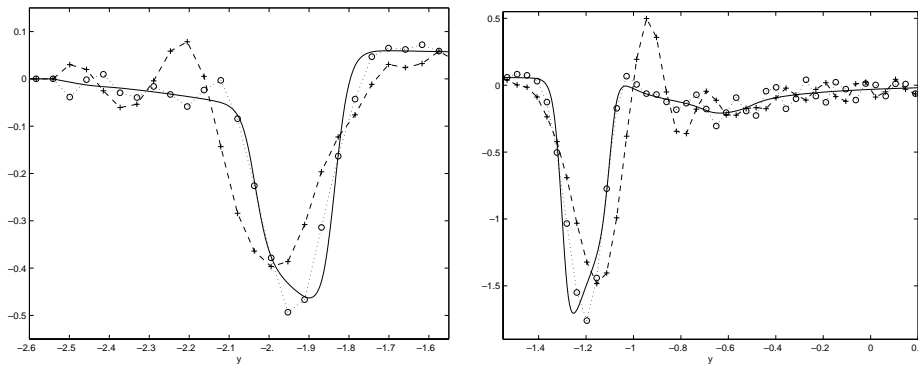


FIG. 10. The bouncing wave solutions for the Dirichlet problem along the line $x = 0$ at $t = 4.41$, centered around $y = -2.1$ (left) and $y = -0.75$ (right). The solid line is the reference solution, and the dashed line with “+” is the second order scheme with $CFL = 0.5$, $N = 100$. The dotted line with “o” marks the fourth order scheme with $CFL = 0.1$, $N = 100$. Note that the spurious oscillations are much larger with the second order scheme.

fourth order spatial discretizations. We are currently working on the two-dimensional Neumann problem [7], and we plan to extend the approach to three space dimensions.

For the fourth order spatial discretization, we have seen that the second order temporal discretization error cannot be neglected unless the CFL-number is reduced substantially below the stability limit. In future work we intend to develop a higher order time integration method where the accuracy better matches that of the fourth order spatial discretization.

In many applications the wave propagation speed varies in space. We see no difficulty modifying our approach to handle smoothly varying coefficients, but additional work will be required to treat discontinuous coefficients. Systems of second order wave equations also occur in applications, for example in general relativity. Another example is Maxwell’s equations for electromagnetic wave propagation, which often is given as a first order system, but also can be written as a second order system. We believe that generalizing the proposed method to systems will provide an accurate and straightforward technique for analyzing these types of problems.

REFERENCES

- [1] G. BROWNING, H.-O. KREISS, AND J. OLIGER, *Mesh refinement*, Math. Comp., 27 (1973), pp. 29–39.
- [2] L. COLLATZ, *The Numerical Treatment of Differential Equations*, 3rd ed., Springer-Verlag, Berlin, 1960.
- [3] A. DITKOWSKI, K. DRIDI, AND J. S. HESTHAVEN, *Convergent Cartesian grid methods for Maxwell’s equations in complex geometries*, J. Comput. Phys., 170 (2001), pp. 39–80.
- [4] T. A. DRISCOLL AND B. FORNBERG, *Block pseudospectral methods for Maxwell’s equations II: Two-dimensional, discontinuous-coefficient case*, SIAM J. Sci. Comput., 21 (1999), pp. 1146–1167.
- [5] B. GUSTAFSSON, H.-O. KREISS, AND J. OLIGER, *Time Dependent Problems and Difference Methods*, Wiley-Interscience, New York, 1995.
- [6] H. JOHANSEN AND P. COLELLA, *A Cartesian grid embedded boundary method for Poisson’s equation on irregular domains*, J. Comput. Phys., 147 (1998), pp. 60–85.
- [7] H.-O. KREISS, N. A. PETERSSON, AND J. YSTRÖM, *Difference Approximations for the Second Order Wave Equation*, Technical report UCRL-JC-145614, Center for Applied Scientific Computing, Lawrence Livermore National Lab, Livermore, CA, 2001.

- [8] R. B. PEMBER, J. B. BELL, P. COLLELLA, W. Y. CRUTCHFIELD, AND M. WELCOME, *An adaptive Cartesian grid method for unsteady compressible flow in irregular regions*, J. Comput. Phys., 120 (1995), p. 278–304.
- [9] B. STRAND, *Simulations of acoustic wave phenomena using high-order finite difference approximations*, SIAM J. Sci. Comput., 20 (1999), pp. 1585–1604.
- [10] R. WELLER AND G. H. SHORTLEY, *Calculation of stresses within the boundary of photoelastic models*, J. Appl. Mech., 6 (1939), pp. A71–A78.
- [11] C. ZHANG AND R. LEVEQUE, *The immersed interface method for acoustic wave equations with discontinuous coefficients*, Wave Motion, 25 (1997), pp. 237–263.